Structure formation and phase transitions in Gibbs and Langmuir monolayers of amphiphilic acid amides

V. Melzer, D. Vollhardt,* G. Weidemann, G. Brezesinski, R. Wagner, and H. Möhwald
Max-Planck-Institut für Kolloid-und Grenzflächenforschung, Rudower Chaussee 5, D-12489 Berlin, Germany
(Received 9 June 1997; revised manuscript received 22 September 1997)

A comprehensive study of the two-dimensional crystal structure of Gibbs and Langmuir monolayers corroborates recent results that first order phase transition can occur in adsorption layers. The crystal structures and morphological features of the condensed phase of *N-alkyl-γ*-hydroxy-butyric acid amide monolayers with different alkyl chain lengths [*dodecyl* (DHBAA) and *tetradecyl* (THBAA)], but the same head group structure at the air-water interface are investigated. Surface pressure measurements (π-A isotherms for DHBAA and THBAA; π-t adsorption kinetics for DHBAA) are combined with synchrotron x-ray gracing incidence diffraction and Brewster angle microscopy measurements. Twinned domains are formed at lower temperatures ($T<10$ °C) and crosslike domains at higher ($T>10$ °C) temperatures. The oblique crystal structure found in all monolayers is independent of the process of monolayer formation. Macroscopic textures and structures of domains are correlated to the observed crystal structure. The comparison of Gibbs and Langmuir monolayers shows that their crystal structures, morphological textures, and thermodynamic properties are similar. [S1063-651X(98)10101-0]

PACS number(s): 61.10.−i, 68.10.−m, 68.55.−a, 68.70.+w

INTRODUCTION

Processes of ordering and phase transitions in two-dimensional systems have been of recent interest. Such two-dimensional systems formed by amphiphilic molecules at the air-water interface are Gibbs and Langmuir monolayers. While Gibbs monolayers [1] are formed at the surface of aqueous solutions of soluble surfactants by adsorption, Langmuir monolayers of insoluble surfactants [2] are formed at the air-water interface by spreading and compression. It is well known that in Langmuir monolayers first-order phase transitions can occur from a low density fluidlike phase to a condensed phase. The condensed phases can exhibit a large variety of morphological features [3–5] and different crystal structures [6–8]. But for Gibbs monolayers only a few papers [9–13] described the coexistence of two phases in adsorption layers using fluorescence microscopy or Brewster angle microscopy experiments. However, the condensed phase structures observed in these Gibbs monolayers were obviously caused by insoluble or sparingly soluble impurities, or by over saturated solutions of slightly soluble surfactants. In recent papers [14–16], we presented studies on the formation and growth of a condensed phase within the adsorption layer of the amphiphile *N*-dodecyl-*γ*-hydroxy-butyric acid amide (DHBAA) dissolved in the aqueous bulk phase. To understand the ordering processes and the nature of formation of condensed phases in Gibbs monolayers the question of a possible comparison between the structural properties of condensed phases in Gibbs and Langmuir monolayers arises.

Therefore in the present work we compare phase behavior, morphologies, and crystal structures of adsorbed Gibbs monolayers with those of spread Langmuir monolayers of DHBAA and of water insoluble *N*-tetradecyl-*γ*-hydroxy-butyric acid amide (THBAA). The process of phase transition is related to the formation and growth of two-dimensional condensed phase domains in both cases. We are able to visualise the features and growth of these domains using Brewster angle microscopy (BAM). On the other hand, we could investigate the crystal structure of the condensed phases by using synchrotron x-ray gracing incidence diffraction (GIXD). Using these results we compare the crystal structures of Gibbs and Langmuir monolayers. In addition, we will correlate the macroscopic morphology with the microscopic crystal structure to understand processes of ordering in monolayers.

EXPERIMENT

The surfactants DHBAA and THBAA were synthesized by nucleophilic opening of the *γ*-hydroxybutyric acid lactone ring [17]. Thus, equimolar amounts of the corresponding primary amine and *γ*-hydroxybutyric acid lactone were dissolved in dry methanol. The mixture is heated to 80 °C for 5 h in a steel autoclave. The solvent was removed and the crude product recrystallized from *n*-hexane. The chemical purity (>99%) was checked by elemental analysis and HPLC.

The surface pressure (π)–area (A) isotherms and surface pressure (π)–time (t) adsorption isotherms were recorded using a Langmuir film balance (R&K GmbH, Wiesbaden, Germany). The surface pressure was measured by the Wilhelmy method using a small filter paper. The distilled water was made ultrapure by a Milli-Q-system. The Brewster angle microscope (NFT, Göttingen, Germany) was connected with the R&K film balance. For more detailed information about surface pressure measurements and the BAM method, see Refs. [14–16,18,19].

Grazing incidence x-ray diffraction experiments [20–24] were performed using the liquid-surface diffractometer on

*Author to whom correspondence should be addressed.

the undulator beamline BW1 at HASYLAB, DESY, Hamburg, Germany. The Synchrotron beam was made monochromatic by a beryllium (002) crystal and was adjusted to strike the surface at grazing incidence with an angle of incidence $\alpha_i = 0.85\alpha_c$, where α_c is the critical angle for total external reflection. The diffracted radiation was detected by a linear position-sensitive detector (PSD), (OED-100-M, Braun, Garching, Germany) as a function of the vertical scattering angle α_f. A Soller collimator in front of the PSD provided resolution of the horizontal scattering angle $2\Theta_{\mathrm{hor}}$ which is approximately 0.1°. Due to quasielastic scattering, the wave vectors $\mathbf{k}_i$ and $\mathbf{k}_f$ of the incident and the diffracted beams have the same modulus. The scattering vector $\mathbf{Q} = \mathbf{k}_f - \mathbf{k}_i$ has an in-plane component $Q_{xy} = (4\pi/\lambda)\sin(2\Theta_{\mathrm{hor}}/2)$ and an out-of-plane component $Q_z = (2\pi/\lambda)\sin(\alpha_f)$, where $\lambda = 1.364$ Å is the x-ray wavelength. The accumulated position-resolved scans were corrected for polarization, effective area, and powder averaging. The intensities were least squares fitted to model peaks which were taken as the product of a Lorentzian parallel to the water surface with a Gaussian normal to it. Only the lowest order peaks are observed.

From the in-plane diffraction data, it is possible to obtain the lattice spacings

$$d_{hk} = \frac{2\pi}{Q_{xy}^{hk}}, \tag{1}$$

where Q_{xy}^{hk} is the in-plane component of the scattering vector at maximum intensity. The lattice parameters a and b can be calculated from the lattice spacings d_{hk}, and from these the unit cell area A_{xy}.

The tilt angle τ of the long molecular axis with respect to the normal and the lateral tilt direction Ψ_{hk} were calculated from the peak positions of the Bragg rods in the framework of the cylinder model [20]. In the case of an oblique lattice, there are three nondegenerate peaks. In this case, the tilt angle τ can be calculated by solution of the equation system (three equations, one for each hk pair):

$$Q_z^{hk} = Q_{xy}^{hk}\cos\Psi_{hk}\tan\tau. \tag{2}$$

The cross section per chain A_0 is related to the molecular area parallel to the interface A_{xy} and the tilt angle τ:

$$A_0 = A_{xy}\cos\tau. \tag{3}$$

The GIXD measurements of the Gibbs monolayer were started three hours after reaching the inflection point in the adsorption isotherm.

RESULTS

During compression of DHBAA and of THBAA Langmuir monolayers, we observed a pronounced inflection point in the π-A isotherm, and a plateau region which is typical of the first-order phase transition from the low-density fluidlike phase to a condensed phase (Fig. 1), as discussed in detail in Refs. [15,16]. The main phase transition starts with a break in the π-A isotherm at the characteristic points π_C and A_C. As typically observed for such phase transitions, the surface pressure π_C of the main phase transition point increases

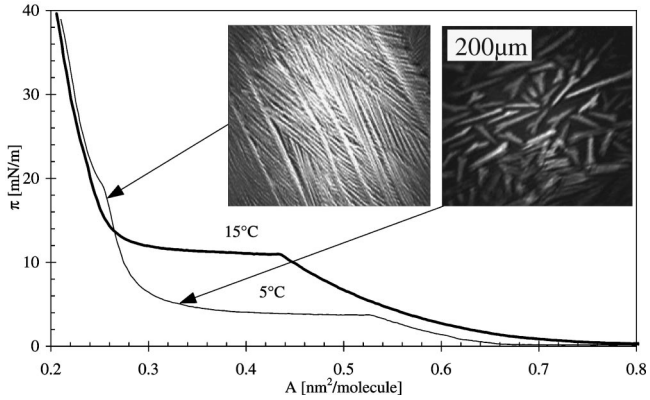

FIG. 1. π-A isotherms of DHBAA at $T = 5$ °C (thin line) and THBAA at $T = 15$ °C (thick line), and corresponding characteristic BAM images of the condensed phase domains. The arrows indicate the position where the BAM images were taken. The scale bar with a size of 200 μm is valid for all BAM images.

($\Delta\pi_C/\Delta T = 1$ mN/m/K) and the size of the related plateau region (change in molecular area between the fluidlike and condensed phase at π_C) decreases with increasing temperature [15,16]. The π-A isotherms of DHBAA Langmuir monolayers, which are slightly soluble in water, were corrected for loss of molecules into the subphase using a reasonable linear correction procedure as described in Ref. [15]. For the water-insoluble THBAA molecules, such a correction was not necessary. The good agreement between the molecular areas of the THBAA and DHBAA π-A isotherms additionally supports the correction for small losses due to dissolution of DHBAA molecules.

In Fig. 1, two typical BAM images are shown for THBAA and DHBAA Langmuir monolayers which confirm the coexistence of two phases, namely fluidlike (dark regions) and a condensed (bright domains) phases. For temperatures below 10 °C, the condensed phase domains of DHBAA have an inner anisotropy and three main growth directions [16]. In contrast, above 10 °C the domains have no inner structure, and exhibit four main growth directions with two typical acute (between 60° and 30°) and obtuse (between 120° and 150°) intersection angles [16].

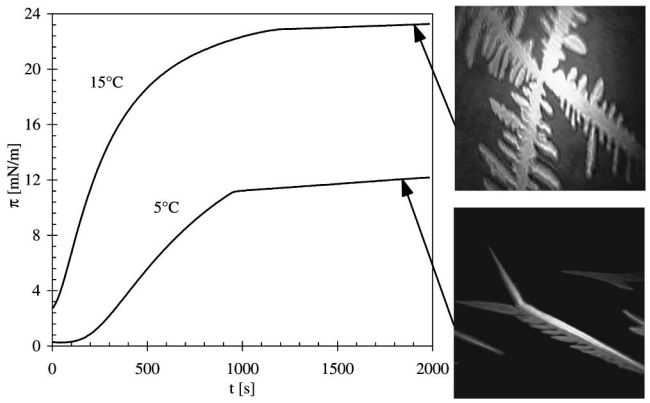

FIG. 2. π-t adsorption isotherms of DHBAA at 5 and 15 °C (bulk concentration of $c = 1.5\times10^{-5}$ mol/dm^3), and characteristic BAM images of Gibbs monolayers of DHBAA in the phase coexistence region. The arrows indicate the temperatures where the BAM images were taken.

FIG. 3. BAM images of a condensed phase domain of a Gibbs monolayer of DHBAA at 15 °C with crossed ($P\perp A$) and parallel ($P\|A$) polarizers. Model of the tilt orientation of the molecules in the domain (bottom).

TABLE I. Scattering vector components Q_{xy} and Q_z of the diffraction peaks for the Gibbs monolayer of DHBAA at 5 and 15 °C, and their full width at half-maximum (ΔQ_{xy} and ΔQ_z).

π (mN/m)	T (°C)	Q_{xy} (10) (1/Å)	Q_z (10) (1/Å)	Q_{xy} (01) (1/Å)	Q_z (01) (1/Å)	Q_{xy} ($1\bar{1}$) (1/Å)	Q_z ($1\bar{1}$) (1/Å)
21	5	1.442	0.031	1.380	0.73	1.473	0.70
25	15	1.451	0.006	1.382	0.69	1.472	0.66
π (mN/m)	T (°C)	ΔQ_{xy} (10) (1/Å)	ΔQ_z (10) (1/Å)	ΔQ_{xy} (01) (1/Å)	ΔQ_z (01) (1/Å)	ΔQ_{xy} (11) (1/Å)	ΔQ_z (11) (1/Å)
21	5	0.007	0.22	0.018	0.25	0.016	0.27
25	15	0.006	0.2	0.007	0.25	0.011	0.27

During the formation of an adsorbed Gibbs monolayer of DHBAA molecules, we have also observed an inflection point, indicative of a phase transition, in the π-t adsorption isotherms which is more pronounced at lower temperatures (Fig. 2) [14–16]. In Fig. 2, two typical BAM images of DHBAA Gibbs monolayers are additionally shown to illustrate the coexistence of two phases above π_C in the π-t adsorption isotherms. The low-density fluidlike phase is represented by dark regions, and the condensed phase by the bright domains. The domains are formed above π_C, and reach a size visible by BAM after an induction period. Below 10 °C the domains have three main growth directions, and are subdivided into two sections with different azimuthal chain tilt orientation along the two homogeneously reflecting growth directions [14]. These condensed phase domains are directly comparable with those of Langmuir monolayers (compare Fig. 2 with Fig. 1). Above 10 °C, the condensed phase domains grow in four main growth directions with the same typical acute and obtuse intersection angles as observed for Langmuir monolayers. By varying the analyzer position the orientation of molecules in the domains can be

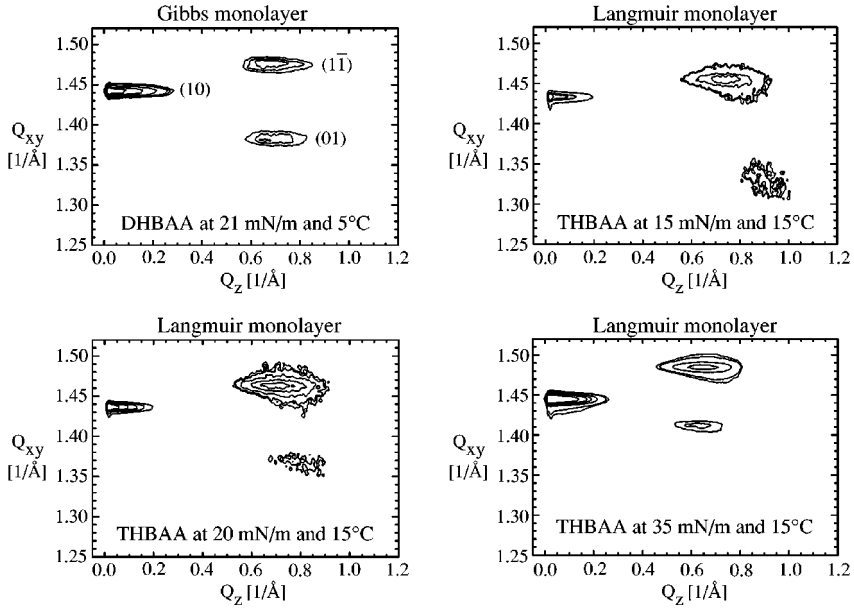

FIG. 4. Contour plots of a Gibbs monolayer of DHBAA ($\pi = 21$ mN/m, $c = 2\times10^{-5}$ mol/dm^3, and $T = 5$ °C) and of a Langmuir monolayer of THBAA ($\pi = 15$, 20, and 35 mN/m, and $T = 15$ °C).

TABLE II. Scattering vector components Q_{xy} and Q_z of the diffraction peaks for the Langmuir monolayer of THBAA at 15 °C, and their full width at half-maximum (ΔQ_{xy} and ΔQ_z) at different surface pressures.

π (mN/m)	T (°C)	Q_{xy} (10) (1/Å)	Q_z (10) (1/Å)	Q_{xy} (01) (1/Å)	Q_z (01) (1/Å)	Q_{xy} $(1\bar{1})$ (1/Å)	Q_z $(1\bar{1})$ (1/Å)
8	15	1.407	0.01	1.303	0.90	1.440	0.88
12	15	1.408	0.02	1.315	0.87	1.448	0.85
15	15	1.434	0.03	1.335	0.82	1.455	0.77
20	15	1.437	0.02	1.360	0.75	1.463	0.73
35	15	1.445	0.03	1.412	0.65	1.486	0.67
π (mN/m)	T (°C)	ΔQ_{xy} (10) (1/Å)	ΔQ_z (10) (1/Å)	ΔQxy (01) (1/Å)	ΔQ_z (01) (1/Å)	ΔQ_{xy} (11) (1/Å)	ΔQ_z $(1\bar{1})$ (1/Å)
8	15	0.026	0.42	0.05	0.41	0.04	0.37
12	15	0.030	0.38	0.05	0.40	0.04	0.30
15	15	0.009	0.26	0.05	0.29	0.024	0.29
20	15	0.008	0.23	0.038	0.27	0.026	0.25
35	15	0.009	0.23	0.023	0.29	0.017	0.24

deduced. For parallel polarizers the domain with the longest growth direction parallel to the plane of beam incidence, which is horizontal for these BAM images, was clearly visible with the same brightness (Fig. 3, middle). In contrast, the domain was not visible when the polarizers are crossed (Fig. 3, top). The domains do not exhibit any inner anisotropy. Therefore, we must assume a chain tilt parallel to the longest growth direction. In this case, when the longest growth direction is parallel to the plane of beam incidence, the molecules reflect only linear polarized light parallel to this plane. As a result, the domain is not visible when the polarizers are crossed, because the analyzer is perpendicular to the plane of beam incidence. The schematic representation of the tilt direction of molecules in isotropic domains with four growth directions is shown in Fig. 3 (bottom).

Finally we have done GIXD measurements on Gibbs monolayers of DHBAA and Langmuir monolayers of THBAA in order to compare the monolayer types and their crystal structures. The contour plots of the corrected diffraction intensities as a function of the in-plane (Q_{XY}) and out-of-plane (Q_Z) components of the scattering vector for adsorbed Gibbs monolayers of DHBAA and compressed Langmuir monolayers of THBAA at different surface pressures are presented in Fig. 4. The positions of the peak maxima and their full widths at half-maximum are listed in Table I for the Gibbs monolayer of DHBAA, and in Table II for the Langmuir monolayer of THBAA.

TABLE III. Lattice parameters of the condensed phase formed in the adsorbed Gibbs monolayer of DHBAA at 5 and 15 °C. (a)–(c) Lattice dimensions. γ is the angle between the [10] (a axis) and [01] (b axis) directions, A_{xy} is the unit cell area per molecule, τ is the tilt angle of the molecules with respect to the normal, A_0 is the chain cross section, and Ψ_a is the azimuthal tilt angle of molecules with respect to the [10] direction (a axis).

π (mN/m)	a (Å)	b (Å)	c (Å)	A_{xy} (Å^2)	A_0 (Å^2)	γ [°]	Ψ_a [°]	τ [°]
21 (5 °C)	4.895	5.115	5.227	22.3	19.2	117.1	114.9	30.3
25 (15 °C)	4.881	5.123	5.196	22.2	19.4	117.5	115.3	28.9

TABLE IV. Lattice parameters of the condensed phase in the Langmuir monolayers of THBAA at 15 °C and different surface pressures. The symbols are as in Table III.

π (mN/m)	a (Å)	b (Å)	c (Å)	A_{xy} (Å^2)	A_0 (Å^2)	γ [°]	Ψ_a [°]	τ [°]
8	4.966	5.362	5.489	23.9	19.0	115.9	115.1	37.3
12	4.957	5.309	5.460	23.7	19.2	115.8	114.7	36.1
15	4.906	5.270	5.344	23.1	19.1	116.8	114.2	34.0
20	4.907	5.185	5.278	22.7	19.3	117.0	115.7	31.6
35	4.896	5.010	5.153	21.8	19.3	117.3	119.3	27.7

The indexing of the diffraction peaks to lattice planes, which was used for calculation of lattice parameters, is marked in the contour plot of DHBAA Gibbs monolayer (Fig. 4). The same indices of the diffraction peaks were used for the THBAA Langmuir monolayer. This was reasonable due to the comparable position of the observed diffraction peaks. It is important to note that for higher surface pressures (above $\pi = 15$ mN/m) the full width at half-maximum of the horizontal scattering vector component which is a measure of the positional correlation length ξ of the (10) diffraction peak, was very small and resolution limited, whereas all other peaks had a broader full width at half-maximum which was significantly above the resolution limit of $\Delta Q_{XY} = 0.01$ Å^{-1}.

From the positions of the peak maxima one can calculate the crystal structure at each surface pressure. The resulting lattice parameters of the condensed phases of the monolayers are listed in Table III for the Gibbs monolayer of DHBAA, and in Table IV for the Langmuir monolayer of THBAA. The condensed phases of both DHBAA and THBAA monolayers exhibit an oblique lattice structure of strongly tilted molecules ($\tau > 27°$). The tilt direction of molecules is nearly parallel to the b axis of the unit cell at all surface pressures measured (Fig. 5).

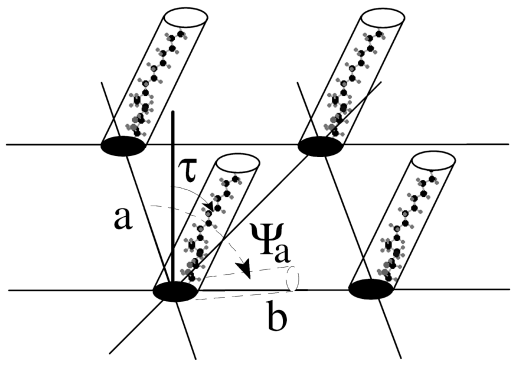

FIG. 5. Model of the crystal structure of an oblique lattice with the tilt direction of the molecules almost parallel to the b axis of the unit cell. The size of the molecules is not reduced by the same proportion.

DISCUSSION

In our first studies [14–16] on thermodynamic behavior, formation, and growth of domains of condensed phase in Gibbs (adsorbed) and Langmuir (spread and compressed) monolayers of DHBAA, we showed the occurrence of a first-order transition between fluidlike and condensed phases. The thermodynamical properties and morphological features in Gibbs and Langmuir monolayers were found to be similar. Both monolayer types exhibit different domain textures and shapes at lower ($T<10$ °C) and higher ($T>10$ °C) temperatures. The elongation of the hydrophobic chain (THBAA) decreases the lateral pressure π_C of the phase transition. The temperature dependence of π_C is the same for both compounds. Based on the generic phase diagram for fatty acids [25], one would expect the phase behavior of THBAA to be similar to that of DHBAA at a temperature 18 °C lower. However, BAM experiments have shown that the domain shapes of THBAA, observed between 5 and 30 °C, are similar to those of DHBAA at higher temperatures. Only domains with four main growth directions and dentritic growth pattern were observed.

Due to the very slow growth process of condensed phase domains in Gibbs monolayers, the tip shape of growing domains is rounder compared to that in Langmuir monolayers. This is in good agreement with theoretical calculations, which have shown that the tip shape and tip splitting are related to the degree of deviation from equilibrium [26,27].

X-ray diffraction experiments (GIXD) provided information about the structural properties of condensed phases in Gibbs and in Langmuir monolayers. Since X-ray diffraction of Langmuir monolayers is well characterized, this comparison can be used to understand ordering processes and the nature of formation of condensed phases in Gibbs monolayers. In both types of monolayers we have found an oblique lattice structure with large tilt angles of molecules and an azimuthal tilt direction of alkyl chains almost parallel to the *b* axis, as shown in Fig. 5. Although an increase in temperature changes the domain shapes in Gibbs monolayers, the diffraction patterns remain qualitatively unchanged. As is already known for Langmuir monolayers, the cross-sectional area increases with increasing temperature in Gibbs monolayers as well (Table III).

In the Langmuir monolayers the usual dependence of the tilt angle on surface pressure was observed, that is the tilt angle decreases with increasing lateral pressure. The axis close to the direction of the tilt (*b* axis) also decreases with increasing pressure, whereas the *a* axis of the unit cell changes only slightly. The small cross-sectional area A_0 of the molecules of both monolayer types is indicative of a crystalline packing. Here A_0 is smaller than that of fatty acids [28]. The crystal structure is obviously independent of the process of monolayer formation. There is no indication in either type of monolayer of the formation of three-dimensional clusters or aggregates, which would be indicated by additional diffraction peaks.

As observed in other cases, the positional correlation length is largest parallel to the direction of a directed bond [29]. Also, the pressure dependence of the spacings parallel to this bond is significantly smaller. Therefore, the formed hydrogen bondings between the acid amid groups are assumed to be parallel to the *a* axis (Fig. 5). In addition, the dimension of the *a* axis is in the range of 4.9 Å, which is the typical distance for hydrogen bondings between amide groups [30,31]. The lattice spacings of the *b* and *c* axes are significantly larger. Both results are in good agreement with the observed three-dimensional crystal structure of comparable amphiphilic acid amide compounds [31,32].

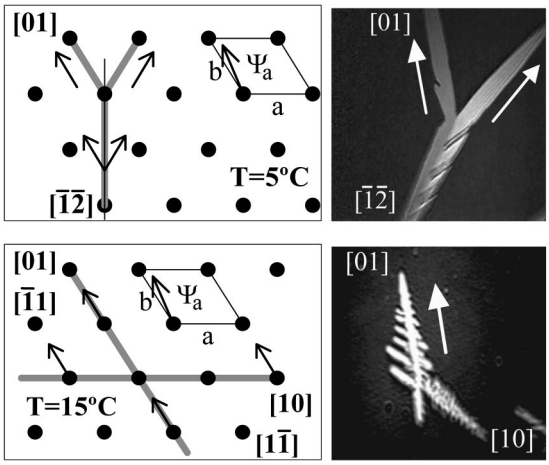

FIG. 6. Correlation of crystal structure (left) with domain structure (right) for lower ($T=5$ °C, top) and higher ($T=15$ °C, bottom) temperatures. The positions of the molecules are represented by filled circles. The thick grey lines in the crystal structure illustrate the growth directions in the domains. The arrows symbolize the azimuthal tilt direction of the molecules. A scheme of the unit cell is inserted.

The full widths at half-maximum of in-plane scattering vector components of the (11) and (01) reflexes of the Gibbs monolayer are significantly smaller compared to those of the Langmuir monolayer. Consequently, the density of defects is smaller in the Gibbs monolayer due to the slower and more homogeneous growth process of condensed phase domains during adsorption. This is in agreement with the domain morphology observed with BAM.

It should be possible to correlate macroscopic features with the microscopic crystal structure of monolayers [33]. Using the models of domains proposed for lower [14] and higher temperatures (Fig. 3), we can correlate the main or preferred growth directions of dendritic domains with the low indexed lattice directions (Fig. 6). Accordingly, the preferred growth directions are parallel to the [01] and [1 2] lattice directions for the lower temperature case ($T=5$ °C). The bisector of the main domain is consequently parallel to the [1 2] lattice direction. For the higher temperature case ($T=15$ °C) the growth directions are parallel to the [01] and [10] lattice directions for intersection angles between growth directions of about 120° and parallel to the [11] and [10] lattice directions for intersection angles between growth directions of about 150°. It is important to note that the low and high temperature domain shapes can be described by the same lattice structure.

van der Waals interactions between alkyl chains are isotropic, and result in an isotropic growth of condensed phase domains, as observed for fatty acids [34] and fatty alcohols [35]. From morphological features and crystal structures of the investigated Gibbs and Langmuir monolayers, we conclude that the observed dendritic growth in preferred direc-

tions is a result of the anisotropy of the hydrogen bonding between acid amide groups, which obviously has a stronger influence on the domain morphology than the interaction between the chains.

CONCLUSIONS

In summary, the present work provides additional evidence for the recent finding of a first-order phase transition in adsorption layer, so far completely discounted in the field of adsorption and adsorption kinetics. In recent work [14–16], first-order phase transition was concluded from an inflection point in the $\pi(t)$ adsorption kinetics, and visualized using Brewster angle microscopy. The comprehensive characterization of the features of the condensed phase of an adsorption layer provides insight into the molecular packing properties of the adsorption layers.

The GIXD data obtained for the adsorption layers corroborate recent results that condensed phase structures are formed in adsorption layers. The results of the lattice structure indicate that real crystalline structures can be formed in adsorption layers. Gibbs adsorption layers of DHBAA were found to produce time-stable, crystalline two-dimensional (2D) monolayers.

A second 2D texture of the DHBAA monolayers found in a higher temperature region and its microscopic orientational order was analyzed. The 2D crystal structures can be correlated with the preferred growth directions of both 2D modifications of the domain texture. For a comparison with sparingly soluble Langmuir monolayers, the longer chain homologous *N*-alkyl-γ-hydroxybutyric acid amide (THBAA) was prepared and thermodynamically, morphologically, and structurally characterized. The crystal structures, morphological features, and thermodynamic properties of both the Langmuir and Gibbs monolayers were found to be similar. It has been shown for DHBAA and THBAA monolayers that the strong hydrogen bonding between acid amide groups is responsible for the formation of a dendritic crystalline condensed monolayer phase.

The experimental finding of a first-order phase transition in adsorption layers has general consequences for the field of adsorption and adsorption kinetics. In particular, the theoretical description of adsorption and adsorption kinetics has to be modified under the consideration of a first-order phase transition.

ACKNOWLEDGMENTS

Financial assistance from the Deutsche Forschungsgemeinschaft (Sfb 312) and the Fonds der Chemischen Industrie is gratefully acknowledged. We have to thank Dr. B. Struth for his help during the x-ray diffraction measurements, and Dr. C. E. DeWolf for helpful discussions. We thank HASYLAB at DESY for providing excellent facilities and financial support.

[1] A. W. Adamson, *Physical Chemistry of Surfaces*, 5th ed. (Wiley, New York, 1990).
[2] G. L. Gaines, *Insoluble Monolayers at Liquid-Gas Interfaces* (Interscience, New York, 1966).
[3] C. M. Knobler, Science **240**, 870 (1990).
[4] H. Möhwald, Rep. Prog. Phys. **56**, 653 (1993).
[5] D. Vollhardt, Adv. Colloid Interface Sci. **64**, 143 (1996).
[6] A. M. Bibo, C. M. Knobler, and I. R. Peterson, J. Phys. Chem. **95**, 5591 (1991).
[7] E. Scalas, G. Brezesinski, H. Möhwald, V. M. Kaganer, W. G. Bouwman, and K. Kjaer, Thin Solid Films **284/285**, 56 (1996).
[8] V. Melzer, G. Weidemann, D. Vollhardt, G. Brezesinski, R. Wagner, B. Struth, and H. Möhwald, Supramol. Sci. **4**, 391 (1997).
[9] B. Berge, L. Faucheux, K. Schwab, and A. Libchaber, Nature **350**, 322 (1991).
[10] J. M. Flesselles, M. O. Magnasco, and A. Libchaber, Phys. Rev. Lett. **67**, 2489 (1991).
[11] S. Hénon and J. Meunier, Thin Solid Films **210/211**, 121 (1992).
[12] S. Hénon and J. Meunier, J. Chem. Phys. **98**, 9148 (1993).
[13] S. Rivière, S. Hénon, and J. Meunier, Phys. Rev. E **49**, 1375 (1994).
[14] V. Melzer and D. Vollhardt, Phys. Rev. Lett. **76**, 3770 (1996).
[15] V. Melzer and D. Vollhardt, Prog. Colloid Polym. Sci. **103**, 130 (1997).
[16] D. Vollhardt and V. Melzer, J. Phys. Chem. B **101**, 3370 (1997).
[17] J. Houben and Th. Weyl, *Methoden der Organischen Chemie* (G. Thieme Verlag, Stuttgart, 1957), Vol. XI/1, p. 328.
[18] D. Hönig, G. A. Möbius, and D. Möbius, J. Phys. Chem. **95**, 4590 (1991).
[19] S. Hénon and J. Meunier, Rev. Sci. Instrum. **62**, 936 (1991).
[20] J. Als-Nielsen, in *Structure and Dynamics of Surfaces*, edited by W. Schommers and P. von Blanckenhagen (Springer-Verlag, Berlin, 1986), Vol. 2.
[21] J. Als-Nielsen and K. Kjaer, *Phase Transitions in Soft Condensed Matter, NATO Advanced Study Institute Series B: Physics*, edited by T. Riste and D. Sherrington (Plenum, New York, 1989).
[22] K. Kjaer, Physica B **198**, 100 (1994).
[23] J. Als-Nielsen, D. Jaquemain, K. Kjaer, M. Lahar, F. Leveiller, and L. Leiserowitz, Phys. Rep. **246**, 251 (1994).
[24] J. Als-Nielsen and H. Möhwald, in *Handbook on Synchrotron Radiation*, edited by S. Ebrashi, M. Koch, and E. Rubenstein (Elsevier, Amsterdam, 1991).
[25] V. M. Kaganer, I. R. Peterson, R. M. Kenn, M. C. Shih, M. Durbin, and P. Dutta, J. Chem. Phys. **102**, 9412 (1995).
[26] A. Gliozzi, A. C. Levi, M. Menessini, and E. Scalas, Physica A **203**, 347 (1994).
[27] G. Indiveri, A. C. Levi, A. Gliozzi, E. Scalas, and H. Möhwald, Thin Solid Films **284/285**, 106 (1996).
[28] R. M. Kenn, C. Böhm, A. M. Bibo, I. R. Peterson, H. Möhwald, J. Als-Nielsen, and K. Kjaer, J. Phys. Chem. **95**, 2092 (1991).
[29] S. P. Weinbach, D. Jacquemain, F. Leveiller, K. Kjaer, J. Als-Nielsen, and L. J. Leiserowitz, J. Am. Chem. Soc. **115**, 11 110 (1993).

[30] L. Leiserowitz and A. T. Haglar, Proc. R. Soc. London, Ser. A **388**, 133 (1983).
[31] R. Rudert, Y. Wu, and D. Vollhardt, Z. Kristallogr. **211**, 114 (1996).
[32] R. Rudert, Ch. André, R. Wagner, and D. Vollhardt, Z. Kristallogr. **212**, 752 (1997).
[33] G. Brezesinski, E. Scalas, B. Struth, H. Möhwald, F. Bringezu, U. Gehlert, G. Weidemann, and D. Vollhardt, J. Phys. Chem. **99**, 8758 (1995).
[34] C. M. Knobler, Adv. Chem. Phys. **77**, 397 (1990).
[35] S. Siegel and D. Vollhardt, Colloids Surf., A **116**, 195 (1996).